# NAVAL RESEARCH REVIEWS

NOVEMBER 1978



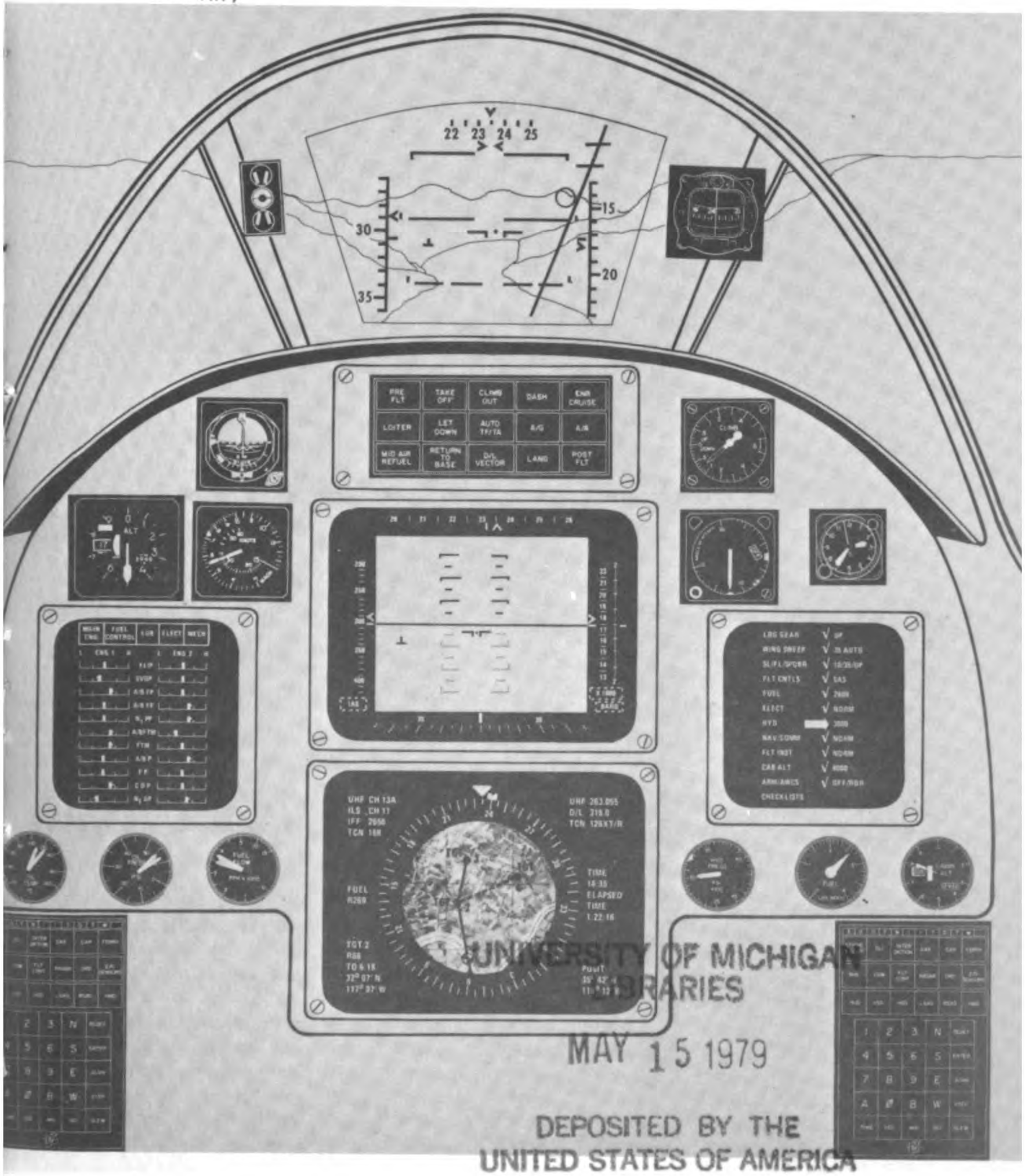

# PROFILES IN SCIENCE

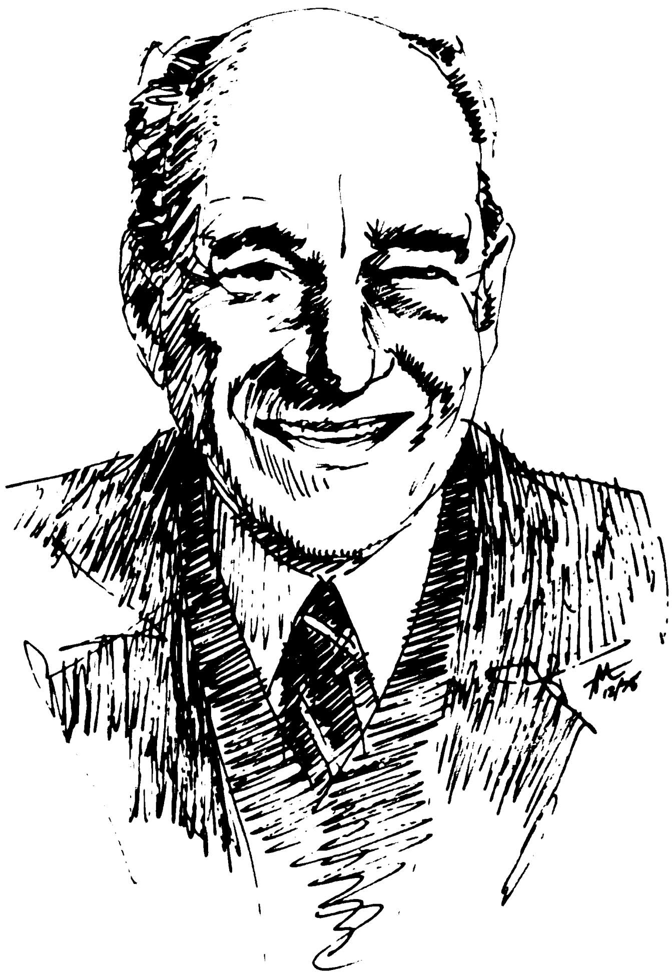

*Professor August J. Durelli*

Professor August J. Durelli is the John F. Dodge Professor of Engineering at Oakland University Dr. Durelli, who is a native of Buenos Aires, came to the United States in 1946 working first at the Armour Research Foundation and later holding Professorships at Illinois Institute of Technology and Catholic University of America.

Professor Durelli is an outstanding scientist in the field or experimental mechanics where he is known for pioneering research in the areas of photoelasticity, the brittle material and brittle coating methods of stress analysis, holography, and dynamic stress analysis. For many years Professor Durelli has been a contractor for the Office of Naval Research investigating stresses and strains in solid propellant rocket grains and cases, shockwaves in soils, and failure of jet engine turbine blades and buckets. He is a Fellow of the New York Academy of Sciences and the American Society of Mechanical Engineers.

# The Measurement of Residual Stresses with X-Rays

**J.B. Cohen and M.R. James**
*The Technological Institute*
*Northwestern University*
**and**
**B.A. MacDonald***
*Office of Naval Research*

### Introduction

Because of the importance of residual stresses in affecting the life of naval structural components, the Metallurgy and Ceramics Program of the Office of Naval Research has supported research on improving residual stress measuring techniques. This program has emphasized the X-ray method of measuring stresses, concentrating on three primary objectives- rapid measurement capability, high accuracy, and ease in equipment portability. For industrial production line uses the first two goals are desirable, especially for monitoring of residual stresses as a nondestructive check on product quality and reliability. The importance of portability is clear when considering possible field use of a stress measuring device in aircraft and shipyard environments. Checking stresses during construction of structures such as welded ship hull sections requires a highly portable X-ray device with simple setup procedures.

This article describes the Office of Naval Research sponsored effort at Northwestern University under Professor Jerry Cohen. Because of this support Professor Cohen and his associates have been successful in streamlining X-ray stress measurement procedures by incorporating automated control. They have developed techniques that provide improved stress measuring accuracy in textured metal alloys. Recently they made a major technical advance by using a position sensitive X-ray detector to replace the conventional proportional counter. This change significantly simplifies stress measurement procedure while reducing the

---

Dr. Cohen is the Engelhart Professor of Material Sciences and Engineering at Northwestern University. His fields of research are phase transformation, clustering, ordering, and deformation.

Dr. James was a Research Assistant under Professor Cohen when he contributed to this paper. Today he is on the staff at Rockwell Science Center, Thousand Oaks, California.

Dr. MacDonald is a Scientific Officer in the Metallurgy and Ceramics Program of the Office of Naval Research. His field of interest is in metal matrix composites.

measurement time. Developing automation and reducing the overall size of the instrument through incorporation of a micro X-ray tube has resulted in a highly portable, handheld stress-measuring device. Stresses can be measured in seconds and X-ray determined values of hardness, grain size and retained austenite (in steels) are possible. The following article reviews the origin of residual stresses in metals, explores various residual stress measuring methods, and describes in detail the recent progress at Northwestern University on stress measurement.

## The Origin of Stresses

Residual stresses can arise in materials in almost every step of processing, as, for example, when a material is subjected to heat treatment or machining. Consider first a material that undergoes no change in crystal structure during heat treatment. If aluminum is cooled quickly from the heat treatment temperature, the surface and the interior contract at different rates, as illustrated in Figure 1a. At some time *A*, this difference coupled with low material yield strength associated with the high temperature induces plastic flow or permanent yielding. The surface regions, which because of the temperature gradient want to contract on cooling more than the interior, are extended by the interior and vice versa. (Note the increase in length near the surface at *A* in Figure 1a.) This is a real effect; for iron-base materials the product of Young's modulus and coefficient of expansion yields a strain of 3.5 MPa (.5 ksi) per°C difference in temperature between two such regions.

On continued cooling to room temperature, point *B*, the surface regions have been extended relative to the interior and consequently end up in compression. These residual surface stresses are important since notches, scratches, sharp changes in cross-section, etc., concentrate any additional applied tensile stresses near the surface and can act to initiate a crack. Residual compressive stresses in the surface must be overcome by the applied load to initiate cracks, and thus the presence of surface compressive stresses is a highly favorable condition.

Heat treatment does not always produce surface compressive stresses. If a material undergoes a phase transformation, as in the hardening of steel to form martensite, the local yielding is essentially masked by the volume expansion associated with the austenite to martensite phase change. The result is illustrated schematically in the cooling curve in Fig. 1b. At temperature *A* the surface regions transform to martensite and expand, since they reach the transformation temperature first. The interior composed of low strength austenite deforms plastically to accommodate this change. At *B* the interior transforms to martensite producing an expansion which is resisted by the high strength martensitic surface. At *C*, near room temperature, the surface is thrown into tension by the interior, producing surface residual tensile stresses, which can contribute to crack initiation and propagation.

Stress relief annealing at moderate temperatures is often employed to allow local yielding to occur thereby minimizing or eliminating such stresses. However, care is needed because even differences in the coefficients of expansion between the carbides and ferrite phases in steel can lead to significant stresses if the parts are not cooled slowly after this treatment.

One way to replace surface tensile stresses with compressive stresses is to shot peen the surface. In this process high velocity shot causes local plastic yielding in the surface which is extended relative to the interior. The interior acts to constrict the surface, resulting in high, local compressive residual stresses in the surface balanced by tensile stresses within the interior, as illustrated in Figure, 1c.

In fact even a tensile extension of a specimen into the plastic region can produce stresses. If the surface is harder than the interior because of defect pileup occurring during plastic extension, then on release of the load (at *A* in Figure 1d), the elastic recovery tries to leave the surface shorter than the interior resulting in surface tensile stresses. The reverse occurs when the surface is softer than the interior. In a forming operation, such as rolling, the surface can be extended more than the interior due to friction at the rolls, as illustrated in Figure 1e, resulting in compression in the surface. In this operation the magnitude of the stress is a function of the thickness of the piece, the roll size and the degree of reduction.[1]

Another important cause of residual stress is welding, as illustrated in Figure 1f. Contraction of molten weld metal during solidification is resisted by colder surrounding metal resulting in the stresses illustrated in the figure. (For further information on stresses in this process see ref. 2.) From these examples (see also refs. 3-5) it is clear that residual stresses in materials arise, not only in processing, but also in use. A rapid, easy-to-use, nondestructive method to measure these stresses is highly desirable. Unfortunately, in too many cases residual stresses are ignored, or it is *assumed* that additional treatment has either eliminated them or introduced compressive stresses. To further complicate the issue macrostresses can develop in different regions of the same piece, and microstresses can arise in microscopic regions, such as between the microscopically-sized phases of a multiphase material. The magnitude of these stresses can be a significant portion (half or more) of the ultimate tensile stress of the annealed material.

## Methods of Measuring Stresses

In view of their importance it is not surprising that there has been a continuing interest in developing methods for measuring residual stresses. In fact over the past four years one or more conferences have been held annually on this subject[6-8]. What is surprising is how seldom these stresses are actually measured and monitored in fabrication or in service!

COOLING CURVES

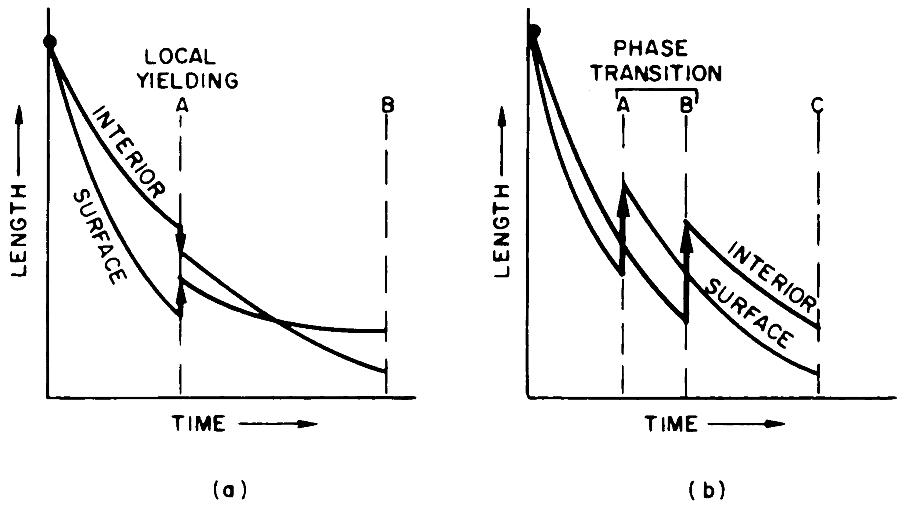


*Figure 1 (a,b) — Schematic cooling curves during a heat treatment showing the difference in contraction of the surface and interior. In (a) there is no phase transition, whereas one occurs in (b).*

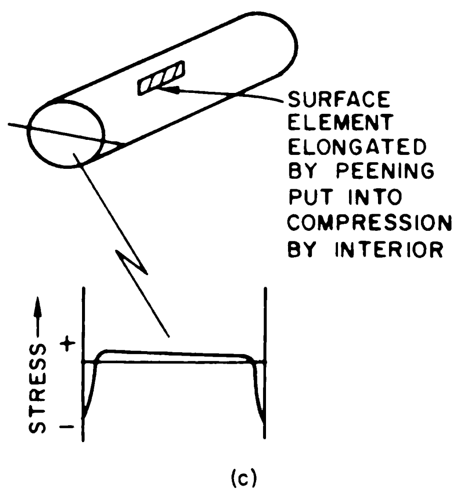


*Figure 1 (c) — Surface deformation by peening elongates surface regions.*

*Figure 1 (d) — The harder surface regions contract more (on release on the load at A) than the softer interior.*

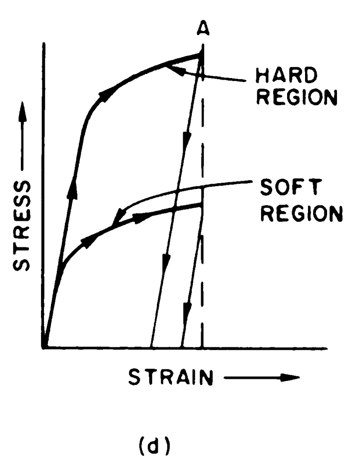

Figure 1 (e) — Friction at the rolls in a rolling mill tends to extend surface regions more than the interior.

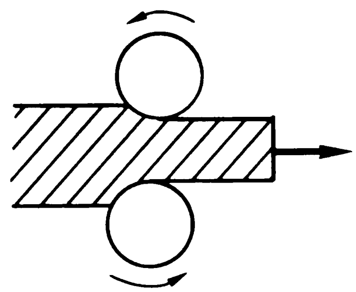

(e)

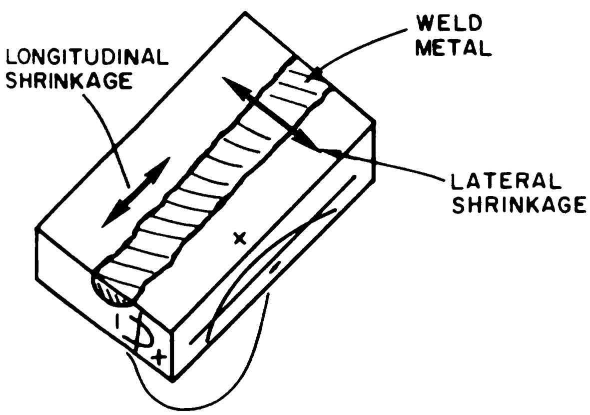


(f)

Figure 1 (f) — Stresses due to welding.

One method for measuring residual stresses in a selected component is to drill a hole and measure subsequent relaxation around the hole (its distortion) with electrical strain gauges. This method is time consuming; great care is needed in making the hole to avoid introducing new stresses and to avoid distortion due to the stress concentrating effects of the hole; and drilling is a destructive method. Futhermore, microstresses cannot be evaluated in this way.[9]

Another technique receiving great interest at the moment is based on acoustic wave propagation.[10] The velocity of a wave in a solid is relatively easy to measure using simple equipment; it depends upon the square root of the elastic constant ($M$). Usually in the elastic region, stress ($\sigma$) and strain $\epsilon$ are written as a proportionality:

$$\sigma = M\epsilon \quad (1)$$

But actually there are higher order elastic constants:

$$\sigma = M\epsilon + C\epsilon^2 + D\epsilon^3 \ldots . \quad (2)$$

Therefore:

$$\sigma \approx (M + C\epsilon)\,\epsilon = M'\epsilon \tag{3}$$

Consequently, the velocity of a wave $V$ is:

$$V = K\,\sqrt{M'} = K\,\sqrt{M + C\epsilon}. \tag{4}$$

The wave velocity depends on the state of strain, $\epsilon$, in the material and hence on the residual stresses. Unfortunately, the distribution of phases present can produce effects that so far have prevented general use of this technique.

Still another stress measuring method is associated with the Barkhausen "noise" in magnetic materials, produced when magnetic domains are moved by a field close to the material(11). This noise is sensitive to the stress fields in the material since the fields affect the ease of rotation of the domains. The measuring equipment is simple, but unfortunately the technique is limited to ferrous alloys. Furthermore, the noise signal saturates at about 350 MPa (50,000 psi) in either tension or compression so the method is most useful, after calibration, for determining the sign of the stress but not its magnitude.

At Northwestern University, under the ONR Metallurgy and Ceramics Program we have been examining the x-ray method for measuring residual stresses. As part of the graduate research program, this support has offered a unique opportunity for performing research with the clear goals of understanding and improving this important nondestructive method.

X-ray methods of measuring residual stresses in crystalline materials have been tested and compared to other methods(12) and are in wide use throughout the world. Manuals have been written for their use in the United States and Japan(13,14). Usually the measurements are made manually on a conventional powder x-ray diffractometer or with a film unit. But there are other units(15) that can make measurements rapidly in 3 to 15 minutes with reasonable precision, and still other devices that are portable to some degree(16).

The basis of the technique is straight forward. First consider the method of x-ray powder diffraction using a single wavelength ($\lambda$) and a flat specimen in a conventional diffractometer. With reference to Figure 2 assume the x-ray detector is moved over a range of angles $2\theta$ to find the largest angle, $\theta$, of the diffraction from grains that satisfies Bragg's law: that is, grains that have planes of atoms with interplanar spacing "*d*" such that $\lambda = 2d \sin\theta$. Grains that have planes with this "*d*" spacing which are parallel to the surface will diffract as shown in Figure 2a. This diffraction takes place from a thin surface layer ($\approx 20\ \mu$m). If the surface of the specimen is in compression, the "*d*" spacing of these planes is larger than in the unstressed state, bacause of Poisson's effect. If the specimen is now tilted with respect to the incoming x-ray beam (Figure 1b) new grains diffract and the orientation of the diffraction planes is more nearly perpendicular to the stress direction.

The result is that with the tilt, the $d$ spacing decreases and the angle $2\theta$ increases, as shown in the figure. In effect the interplanar spacing acts as an internal strain gauge. From isotropic elastic theory the change in $d$ spacing with tilt can be employed to determine the stress $\sigma_\Phi$ in any direction $\Phi$ on the surface[13]:

$$\frac{d_{\Phi,\Psi} - d_o}{d_o} = \epsilon_{\Phi,\Psi} = \left(\frac{1+\nu}{E}\right) \sigma_\Psi \sin^2\Psi + \frac{d_{\Phi,\Psi=0} - d_o}{d_o} \qquad (5a)$$

$$\frac{d_{\Phi,\Psi} - d_{\Phi,\Psi=0}}{d_o} = \left(\frac{1+\nu}{E}\right) \sigma_\Phi \sin^2\psi$$

$$\cong \frac{d_{\Phi,\Psi} - d_{\Phi,\Psi=0}}{d_{\Phi,\Psi=0}}$$

$\Psi$ = specimen tilt,
$d_{\Phi,\Psi}$ = $d$ spacing after specimen tilt $\Psi$,
$d_o$ = stress-free spacing,
$E$ = Young's modulus,
$\nu$ = Poisson's ratio
$\epsilon$ = strain, and
$\sigma$ = stress.

The axial system is shown in Figures 2c and 3. From Eq. (5b) it is clear that the stress $\sigma_\Phi$ can be obtained simply from the slope of $d$ versus $\sin^2\Psi$, if the elastic constants are known. If high accuracy in stress values is desired, it is best to prepare a calibration curve for the material by elastically deforming a specimen of the material under known applied stresses on the diffractometer, because the required elastic constants vary for different diffracting planes and can depend on processing variables. (See Ref. 17 for a recent review of this problem. This procedure is not necessary if only relative values or just the sign of the stress is required.)

Because of the expected linearity of $d$ versus $\sin^2\psi$, many investigators employ just two $\Psi$ angles in the measurement, $\Psi = 0$ and 45 or 60 degrees. This so-called "two-exposure" method reduces the measurement time. From Eq. (5b): $\sigma_\Phi = K(\Delta d/d)$, where $K = E/[(1+\nu)\sin^2\Psi]$. If the stresses are moderate, then from Bragg's law this equation can also be written as $\sigma_\Phi = K'\Delta 2\theta$, where $K' = -(K/2)\cot\theta_{avg}$. A high-angle diffraction peak (from planes of low $d$ spacing) is chosen to give the maximum change in Bragg angle for a given stress and the smallest possible "stress constant" $K'$. For example, for steel one typically employs a (211) diffraction peak, with chromium $K_\alpha$ radiation, and a $\Psi$ tilt of 60 deg. For this case the peak shifts about 0.1 deg $2\theta$ for every $\sim$ 40 MPa (5500 psi) present. In practice it is relatively easy to measure a shift to $\pm$ 0.02 deg $2\theta$.

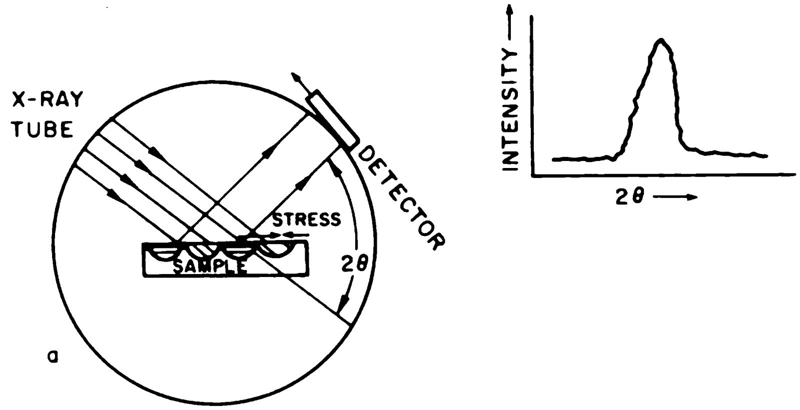


*Figure 2 (a) — Schematic of a diffractometer. The incident beam diffracts x-rays of wavelength λ from planes that satisfy Bragg's law in crystals with these planes parallel to the sample's surface. If the surface is in compression, because of Poisson's ratio these planes are further apart than in the stress-free state. The d spacing is obtained from the peak in intensity versus scattering angle 2θ and Bragg's law, λ = 2 d sin θ.*

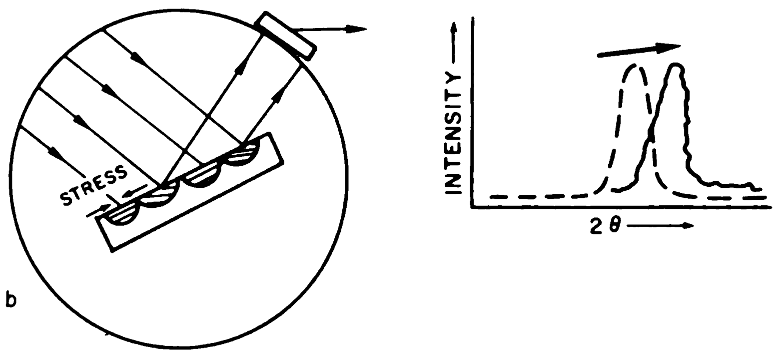


*Figure 2 (b) — After the specimen is tilted, diffraction occurs from other grains, but from the same planes, and these are more nearly perpendicular to the stress. These planes are less separated than in (a). The peak occurs at higher angles of 2θ.*

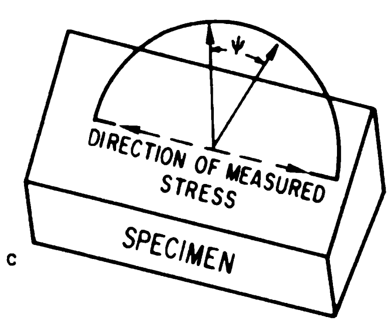


*Figure 2 (c) — After the specimen is tilted, the stress is measured in a direction which is the intersection of the circle of tilt and the surface of the specimen.*

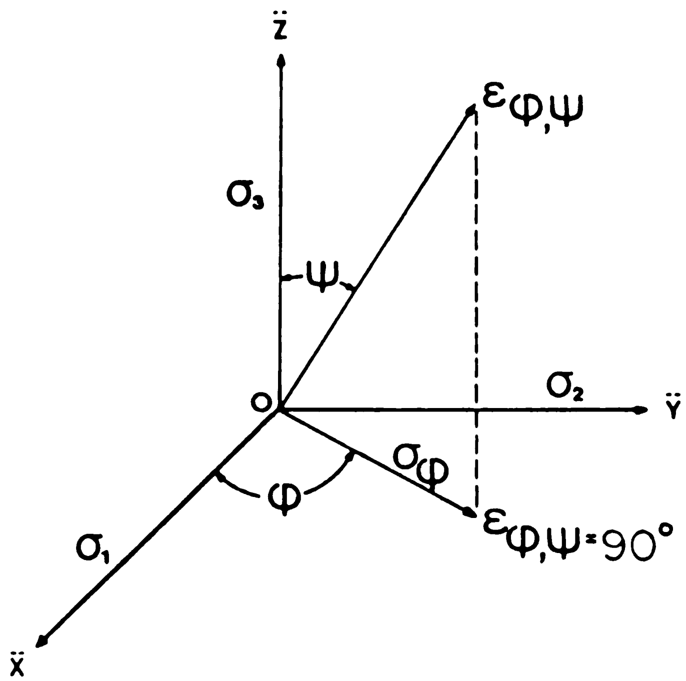


*Figure 3 — Axial system and symbols employed in the equations for stress measurement by x-rays.*

In the initial phase of our research we were concerned about the linearity of *d* vs. $\sin^2\Psi$ that is often assumed. If the stress results from a process that concurrently produces a texture (as in rolling) and the material is single phase (for example, brasses or stainless steels) *d* may not be linear with $\sin^2\Psi$. We developed a simple method for correcting for this nonlinearity that is now used in industry(18).

As the next step in our research we developed a complete automation package for a conventional diffractometer that aligned the specimen, found the peak, and measured enough x-ray counts to determine the stress to an operator-specified precision(19). This package reduced the measurement time on a normal diffractometer from about 45 minutes to 15-20 minutes, and it freed the operator for other work. It permitted us to investigate in systematic fashion the most efficient way to determine stress by allowing repeated measurements. The system parameters were varied and the data scatter examined. For example, it has been common practice in the United States to employ only three diffraction points near the top of a diffraction peak to define it in terms of a parabola. (To locate the center of a diffraction peak of x-ray intensity versus diffraction angle, a parabola is fitted to the data. The center of the parabola defines the Bragg angle and *d*-spacing.) We found that for broad diffraction profiles (large stresses) this method produces twice the scatter that is expected from counting statistics alone, whereas 15 points *measured in the same time* produces only the scatter expected from statistics. There are three basic geometries for stress measurements with x-rays in use today, as illustrated in Figure 4.



290-947 0 - 79 - 2

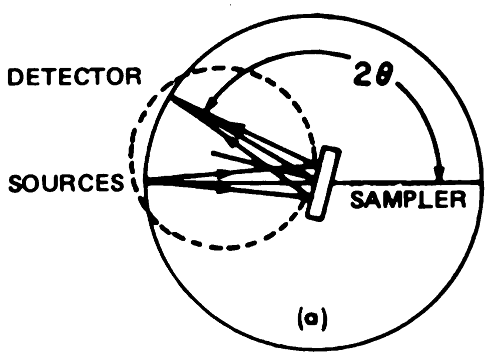


*Figure 4 (a) — The divergent beam usually employed on a diffractometer to expose a wide area on the specimen and still have a sharply focused beam at (D). The source (S), sample, and detector (D) are on a circle (shown dotted) to obtain this focusing.*

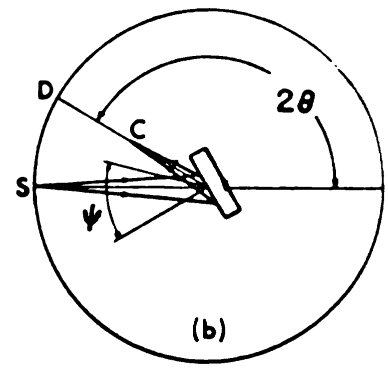


*Figure 4 (b) — When the specimen is tilted ψ deg during a stress measurement the focal point shifts to (C). In the parafocusing method the counter is moved to this new position. In the stationary slit method the detector remains at D.*

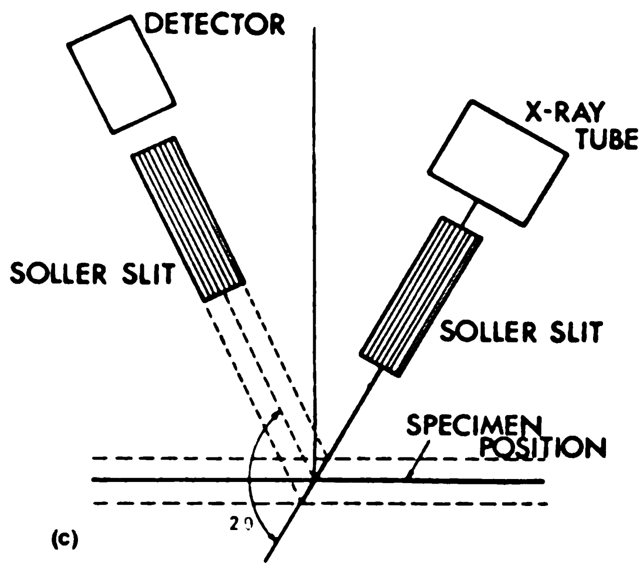


*Figure 4 (c) — Parallel beam geometry. The angle 2θ is defined by the angle between two "Soller" slits (which makes the x-ray beam parallel) and is independent of sample position. (The dashed lines indicate sample positions that would not affect the scattering angle.)*

The parallel beam method is essentially completely free of errors caused by sample position, whereas the stationary slit method has an error of about 14 MPa (2000 psi) for a 0.5 mm sample displacement with a steel specimen[19, 20]. The parafocussing method is *very* sensitive to sample positioning. The first two methods do not produce a sharply focused beam, compared to the parafocussing method; if the peak is sharp, as it often is, there is some broadening (and hence a lowering of intensity at any point near the peak) with the first two techniques. The broadening is less for the stationary slit method than for the parallel beam geometry. This means that for a given counting time the error in locating the peak position is largest for the parallel beam geometry (sometimes by as much as a factor of two)[19,20]. The stationary slit method is a good compromise between speed and reduced sensitivity to errors in sample positioning.

Another x-ray approach that should be mentioned is the "single-exposure method" illustrated in Figure 5. In effect, two tilts are achieved in this method by examining a peak in a powder x-ray pattern from two different sets of grains. This is often done with film, but the error in measured stress caused by a given uncertainty in the peak position is considerably greater than in the other methods (as much as twice), leading to an uncertainty in typical cases greater than that resulting from a 0.5 mm displacement. For these reasons we have decided that the stationary slit-multiple exposure technique is the best.

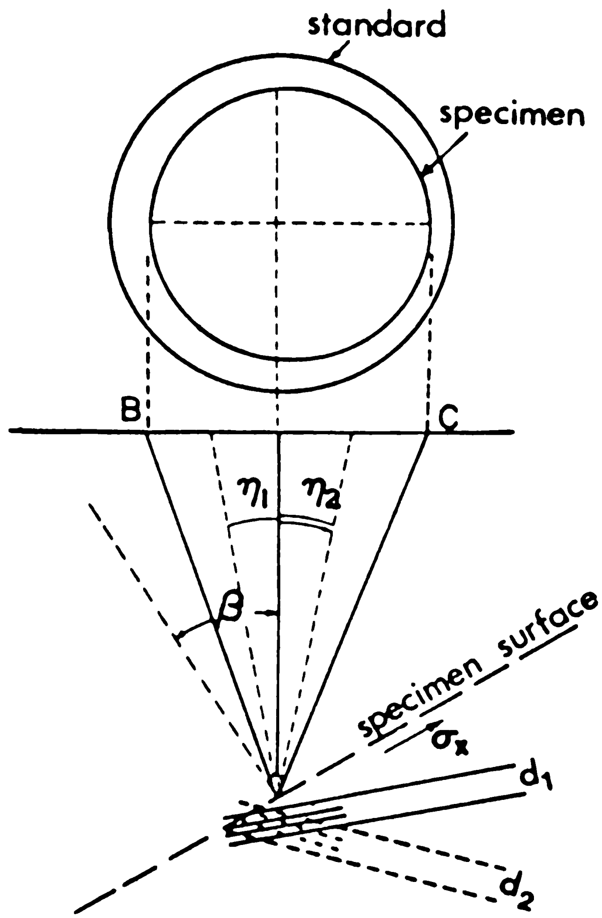


*Figure 5 — The single exposure method. The angles $\eta_1$ and $\eta_2$ are different as they come from different grains with different spacings $d_1, d_2$. A standard powder is often placed on the specimen so that angles can be measured with respect to its diffraction peak. The angle $\beta$ is between the surface normal and the primary beam.*

Having learned as much as we could about the optimum methodology of the technique, we turned our attention to ways of significantly increasing the speed of measurement and the portability of the device. The normal x-ray method is based on recording a diffraction peak by moving the detector around the specimen to record the peak shape, tilting the specimen to one or more $\Psi$ angles, and repeating the process. This is usually done using a conventional diffractometer and requires expensive, heavy gearing. The typical diffractometer also requires bulky transformers and is usually not portable, although instruments mounted on a dolly for transporting in a plant are available. The shortest time of measurement is on the order of minutes.

## "PARS" — A portable X-ray Analyzer for Residual Stresses

Is it necessary to move the detection counter to various points over a diffraction peak to collect the intensity versus angle data? Not if one uses a new x-ray detector called a "position-sensitive detector" (PSD), which is capable of yielding information on both the quality and relative positions of incoming x-ray photons[21]. We used a unit manufactured by Tennelec, Inc., Oak Ridge, Tenn. that employs an argon-3% carbon dioxide gas mixture flowing around a high-resistance graphite-coated wire. When an entering x-ray photon ionizes the gas in the detector, a pulse runs along the wire. By comparing the pulse shape at both ends of the wire, the ionization event can be located to a precision of $\approx 180\mu m$. with suitable electronics, the entire diffraction peak can then be "observed" over several degrees $2\theta$ by means of a multichannel analyzer (MCA). The time differences at both ends are used to locate a single pulse in a channel. Also, the pulse at either end can be summed to allow for energy discrimination. (If the energy is not within prescribed values, storage in the MCA does not occur, which reduces background). The horizontal axis on the MCA is converted to degrees $2\theta$ by calibration with known peaks. Although the detector is flat and not curved to fit a circle around the specimen (as is a diffractometer, see Figure 2) the resulting error is small[20, 22]. For example, for a peak shift of 2 deg. indicating a stress of 1400 MPa (200,000 psi) in steel, the error is only 5 MPa. *With such a device no motion of the counter is needed, eliminating the heavy and expensive gearing of a conventional diffractometer!* The detector employed occupies a volume of 0.2 by 0.13 by 0.045 m, with an active length of 0.1 m. *Because the entire peak is collected simultaneously, the time to measure a stress is reduced by large factors,* 8 *to* 100[19, 23], *the larger value being for sharper peaks.* A least-squares parabolic fit can be made on a micro or miniprocessor to all the data points in the top 15% of the peak (generally 15 to 200 points in that region, the number depending on the peak breadth). All these points are obtained simultaneously in the multichannel analyzer. Peaks can be located with a PSD from ± 0.01 to ± 0.02 deg $2\theta$ by fitting a parabola to the intensity data.

The gas-flow type PSD used in this study can be pressurized for a day's time so that it is not necessary to consider gas supply as part of the design, and sealed units are available, as well. Another important technological advance, the miniature x-ray tube, was adopted to make the instrument portable. We chose one manufactured by Watkins-Johnson Co., Scotts Valley, Calif. The tube is only ≈ 0.06 m long, with its shielding weighs 2.3 kg, and is air-cooled by means of fins. The chromium x-ray target was designed for fluorescence but proved to be adequate for this study. Partly because of the design and partly because of the special grid system employed in the tube's construction, it was found that for the same beam size, at the tube's maximum rating (50 kV, 2mA), the intensity was 20% greater than that from a standard water-cooled x-ray tube operated at 50 kV and 11mA. Furthermore, these miniature tubes are available at ratings up to 5 mA. [In general the data reported here were taken at 40 kV, 1.7 mA. The beam size at the specimen was usually ≈ 0.003 by 0.004 m.]

The basic configuration of PARS[24] is shown in Figure 6a. For the diffraction angle for steel, ≈ 156 deg. $2\theta$, the PSD had to be located behind the x-ray tube. In Fig. 6b, the basic design of the instrument is shown. The detector and tube move on a dovetail track to a stop for a $\Psi$ tilt of 45 deg. For these developmental studies, flat specimens were used and three positioning rods ($A_1$,$A_2$,$A_3$) that were not coplanar were employed to locate the tube-to-specimen distance properly. Other positioning devices are possible for different sample geometries, and the instrument could be readily designed to allow a simple interchange between these. Furthermore, electromagnets or suction pads could be used to hold the position more easily. Only a single calibration experiment is necessary to transform positional data from the PSD into scattering angles.

The prototype instrument being held by one of us (M. J.) is shown in Figure 7. A stand with wheels could also be used to move the instrument from place to place within a plant. There are two grips for PARS that can be seen in the figure, a handle, and a rubber-covered rod for tilting. For safety, a trigger could be incorporated in the handle to start the x-ray tube only if all positioning devices are in place on the specimen. Also, note the plastic back scatter shield for safety.

Figure 8 shows the peaks on the oscilloscope at the two tilts from a steel specimen. One of the interesting additional features of the device is the fact that the entire peak shape is recorded and therefore the breadth is obtained, which is often useful in view of the known empirical relationships between this quantity and hardness. Because of the wide angular range covered by the detector (≈ 20 deg. $2\theta$), peaks from two or more phases can be examined. With different stops along the track for the detector and x-ray tube either stresses in different ma-

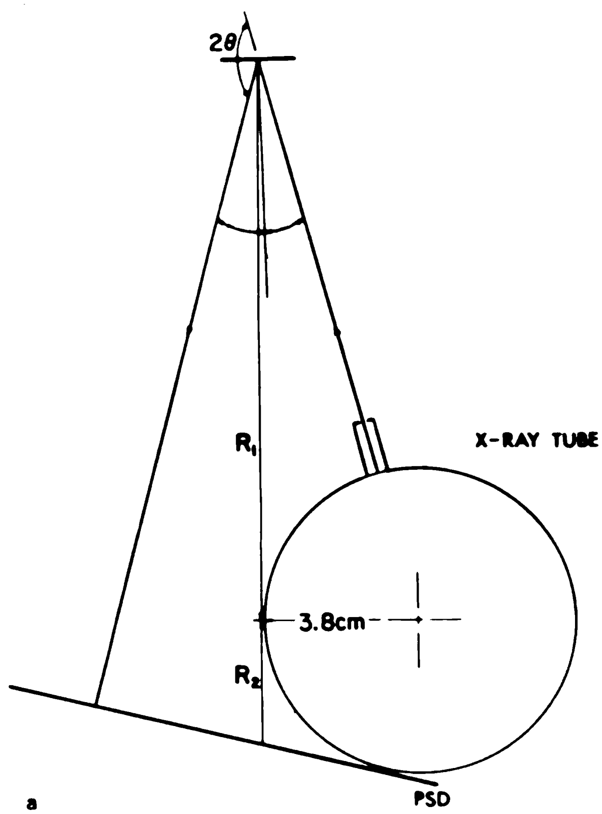


*Figure 6 (a) — Basic configuration of PARS.*

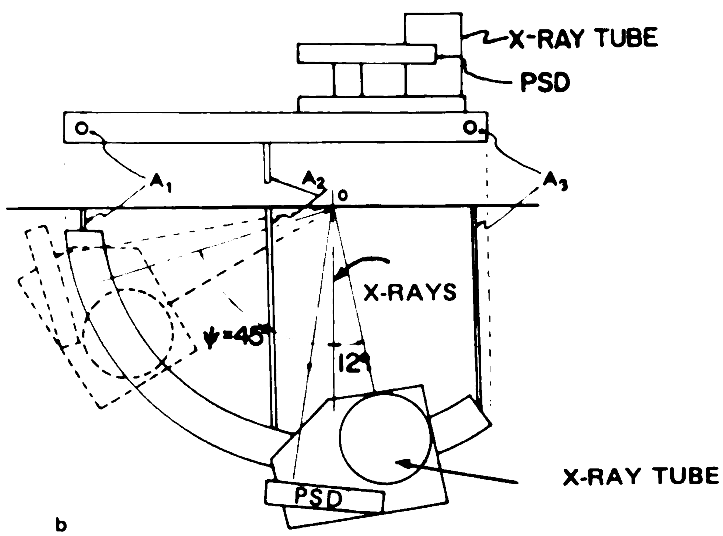


*Figure 6 (b) — Basic design of PARS.*

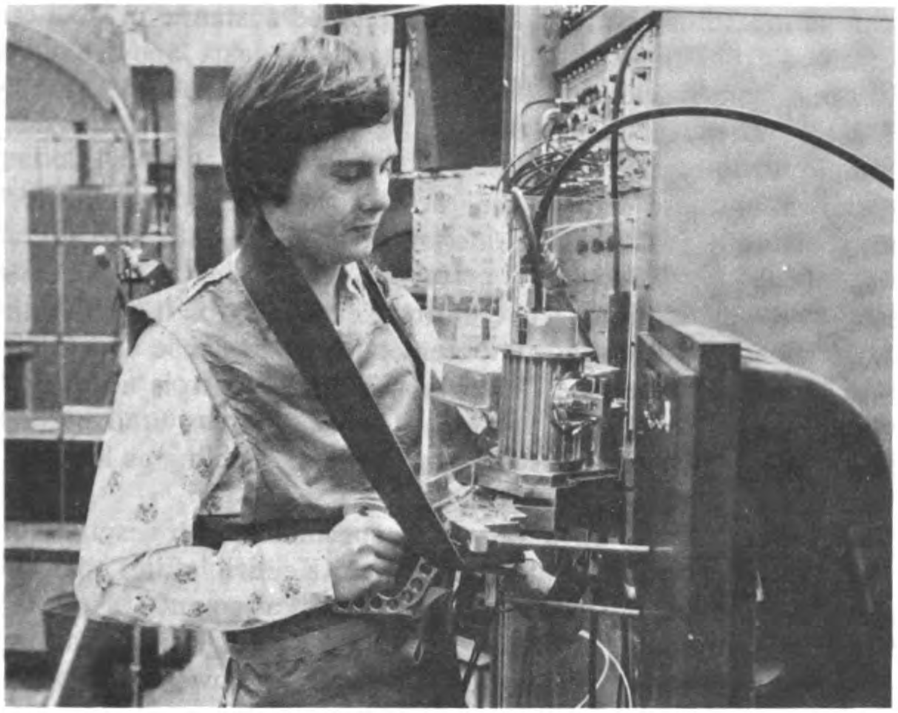

*Figure 7 — The PARS instrument in use by one of the authors (M. J.).*

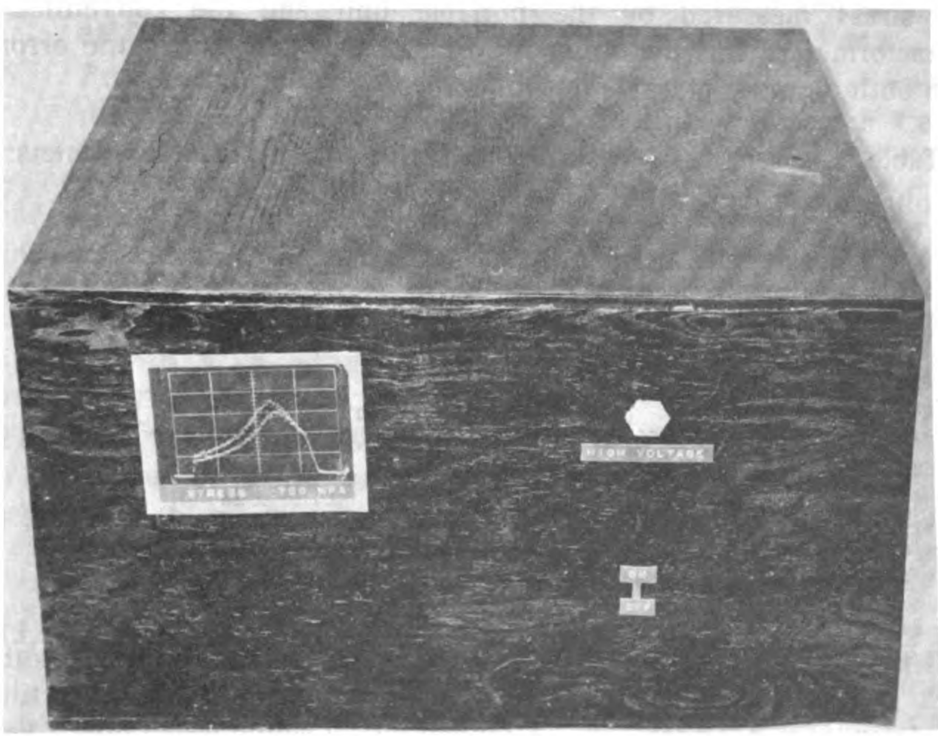


*Figure 8 — The two peaks employed in a stress measurement obtained with PARS, shown on a box that simulates the total electronics package.*

terials can be measured or the quantity of retained austenite in steel can be determined from the ratio of two diffraction peaks, one from the austenite, one from martensite, both recorded simultaneously. Also by moving a specimen rapidly past the beam, the oscillation in intensity can be employed to measure grain size[25].

Not shown in these figures are the associated electronics, which were not specifically packaged for this prototype. The entire x-ray generator is only 0.5 by 0.5 by 0.15 m (about the size of a large digital voltmeter) and weighs 23 kg. The entire electronics for the PSD, the MCA, and a hard-wired microcomputer could be designed into a box 0.5 by 0.5 by 0.2 m as seen in Figure 8. The only controls needed are two switches, of/off and high voltage. The peak stress (and perhaps hardness) could appear on an oscilloscope screen. Cabling as long as 7 m to the portable head is possible.

Table I compares data on a variety of specimens with results from our automated conventional diffractometer. (Keep in mind that this automation alone doubled the usual speed of measurement.) Note that with PARS, measurements at both tilts can be performed in a total time of 4 to 20 seconds, and we did not employ the full power of the tube! The variation observed in five tests on each material is nearly the same as the error resulting from counting statistics, indicating that this error is the only principal one with PARS. (For the sample with the lowest stress there appears to be a difference in both sign and magnitude of the stress measured by the portable unit and the conventional diffractormeter. But the stress is so small that the sum of the errors with both methods brackets this difference.)

Table I — Replicate Measurements with PARS on Steel Specimens; $\psi$ tilt; 45 deg; $CrK_\alpha$ Radiation, (211) reflection

| Steel Sample | Stress with Normal Diffractometer | Average Stress 5 tests with PARS | PARS, Time | Observed Error, 5 tests - PARS | Calculated Statistical Counting Error |
|---|---|---|---|---|---|
| | MPa | MPa | sec | MPa | MPa |
| 1 | +32 | −12 | 10[a] | ±25 | ±20 |
| 2 | −699 | −703 | 20 | ±28 | ±29 |
| 3 | −397 | −396 | 20 | ±43 | ±37 |

a) Measurements to ± 34 MPa counting error in 4 seconds.

The prototype of the portable head weighs about 11 kg, but the tracks are much bulkier than actually needed and the slide for the tube and detector is not necessary. A refined model would weigh only 7 kg.

This device has been demonstrated extensively to industry and is under development for the U.S. Navy. Commercial development has also been initiated and U.S. patent #819,985 has been granted.

In closing, it should be noted that portable x-ray tubes with still greater power are available and xenon filled detectors are about twice as efficient as the one we employed. Thus it is feasible to make measurements in about one second. Also the beam is strong enough to penetrate thin layers of paint or oxide, so that there appear to be minimal problems with its use in the field.

These x-ray methods can also be employed to profile the stress through a part. Unfortunately this involves the removal of material and is therefore destructive; nevertheless, it can be of considerable aid in developmental studies. Clearly one of the great remaining challenges in this area is to devise a simple, quick method of determining stresses vs depth without *damage* to the material.

## References


1. W.M. Baldwin, Jr., Proc. ASTM, **4a**, 539 (1949).
2. V. Papazoglou and K. Masubuchi, Final Technical Report, ONR Contract No. N00014-75-C-0469.
3. G.M. Rassweiller and W.L. Grube (eds.), "Internal Stresses and Fracture in Metals," Van Nostrand Co., New York (1959).
4. O.J. Horger, "Residual Stresses," Metals Eng. Design, ASME Handbook, 2nd ed., McGraw-Hill (1965).
5. F.A. McLintock and A.S. Argon, "Mechanical Behavior of Materials," Addison-Wesley, Reading, Mass. (1966), pp. 420-442.
6. Proceedings of a Workshop on Nondestructive Evaluation of Residual Stress, AFML, NTIAC-76-2, Southwest Research Center, San Antonio, Texas (1976).
7. S. Taira (ed.), "X-ray Study on Strength and Deformation of Metals," The Society of Materials Science, Kyoto, Japan (1971).
8. Harterei-Technische Mitterlungen, **31**, nos. 1 and 2 (1976).
9. R.G. Bathgate, J. Brit. Soc. for Strain Measurement, **4**, no. 2, 20 (1968).
10. G.A. Alers in ref. 6.
11. C.G. Gardner, AMMRC CTR 72-22, Army Materials and Mechanics Research Center, Watertown, Mass., 1972.
12. A.L. Christenson, ed., "The Measurement of Stress by X-rays," SAE Technical Report 182, Society of Automotive Engineers, New York, 1960.
13. M.E. Hilley, ed., "Residual Stress Measurement by X-ray Diffraction," SAE Information Report J784a, Society of Automotive Engineers, New York, Aug. 1971.
14. Committee on Mechanical Behavior of Materials, "Standard Method for X-ray Stress Measurement," The Society of Materials Science, Japan, 1973.

15. E.W. Weinman, J.E. Hunter and D.D. McCormick, Metals Progress, July 1969, p. 88.
16. C.G.R., France; Rigaku-Denki Co., Ltd. Japan; Shimadzu, Ltd., Japan.
17. R.H. Marion and J.B. Cohen, Denver Conf. on Advances in X-ray Analysis, **20**, 355 (1977).
18. R.H. Marion and J.B. Cohen, Denver Conf. on Advances in X-ray Analysis, **18**, 466 (1975).
19. M.R. James and J.B. Cohen, Denver Conf. on Advances in X-ray Analysis, **20**, 291 (1976).
20. M.R. James, Ph.D. Thesis, Northwestern University, Evanston, Illinois, Jan. 1977.
21. C.J. Borkowski and M.K. Kopp, Rev. Sci. Instr. **39**, 1515 (1968).
22. M. James and J.B. Cohen, ONR Technical Report #18, June 15, 1977, Contract No. N00014-75-C-0580.
23. M.R. James and J.B. Cohen, Denver Conf. on Advances in X-ray Analysis, **19**, 697 (1976).
24. M.R. James and J.B. Cohen, Jrnl. of Testing and Evaluation **6**, 91 (1978).
25. W. Paulson, J.B. Cohen and J.E. Hilliard, 15th Sagamore Army Materials Research Conf., Syracuse University Press, N.Y., 1970, p. 73.

## Technique to Laser-Spray Material Surfaces

Two scientists at the Naval Research Laboratory, Drs. Robert J. Schaefer and Jack D. Ayers, report the development of a process for applying coatings to surfaces of materials with high-power lasers.

Among the potential advantages of laser spraying are a more durable and corrosion resistant coating for hardware subjected to extreme environmental conditions than coatings applied by conventional methods.

The more durable surfaces produced by this method on critical components such as high-speed bearings and gas-turbine vanes could lead to substantial reductions in Fleet operating costs.

The new process can be used to apply a wide variety of inorganic coatings, including metals and refractory compounds such as carbides, borides, or oxides to impart desirable protective surface properties without sacrificing bulk structural properties of the substrate.

In carrying out the process, powder of the coating material in injected into the beam of high-energy carbon dioxide ($CO_2$) laser. The intense radiation, which converges to a small spot size on the substrate, heats the powder and propels it rapidly downstream in the form of molten droplets. A thin coating of the powder is applied to the substrate by sweeping the beam over the substrate surface. The research is supported by the Defense Advanced Research Projects Agency (DARPA) and the Office of Naval Research.

# The Development of Integrated Multidimensional Displays

**Robert G. Pachella and Patricia Somers**
*University of Michigan*

## Introduction

The translation of complex quantitative information into a graphic pattern or picture allows for the very efficient communication of that information. With such a symbolic representation an observer can apprehend any or all of the information presented with a single glance. Furthermore, he can perceive directly the relations among the variables being represented. In principle, information about any complex system can be transformed into a picture by simply mapping each of the various aspects of the system into a physical dimension or feature of a visual pattern. The geometric properties of the pattern will then represent the status of the system under observation. The recent availability of computerized graphic devices has now made it feasible to construct such integrated multidimensional displays, thus enabling the presentation of real-time integrations of information about complex systems.

Before displays of this kind can be optimally utilized, however, many questions must be answered about how information should be integrated within the visual displays in order to take advantage of the capabilities of the human perceptual system and to avoid its weaknesses. These questions touch on two of the basic issues in the study of human pattern perception. The first issue concerns the manner in which the physical parameters of the display combine to form spatial configurations. The second asks how these spatial configurations are organized by the observer within his visual field. Questions of this sort have been the focus of research for many years in the study of human perception, but it has only been in the last decade that experimental psychologists have been called upon to translate their general theoretical notions into principles that are specifically useful for the construction of integrated displays. Some of these principles follow straight-forwardly from past research. Others, however, require new research in order to reexamine old concepts with modern techniques.

---

Dr. Pachella is Associate Professor of Psychology and Director of the Human Performance Laboratory at the University of Michigan. He is well known for his research in the field of sensory and perceptual processes. Ms Somers is a Research Assistant at the Human Performance Laboratory.

The research project described here which was supported by ONR attempts to formulate guidelines for the proper construction of complex integrated displays so that they will be maximally compatible with human perceptual abilities.

Consider, for example, the problem of conveying information about a complex system such as a power plant. The variables of interest in such a system include steam outlet temperature and pressure, intake water temperature and flow rate, and electrical demand and generator output. Note that these variables, like those of many complex systems, are interrelated and that decisions and actions dependent upon this information often involve particular correlations between the variables. Thus, the decision to open a particular valve may depend on either steam temperature alone, or pressure alone, or on some correlation between them.

The typical mode of conveying information about these variables is through a panel of instruments or indicators on which each variable is separately displayed. A decision or adjustment to the system based on some combination of the variables would entail mental computation on the part of the observer in order to integrate the relevant information. By contrast, with an integrated display, in which each of the system's variables is mapped into some feature of a geometric pattern or picture, relations among the variables are transformed directly into the spatial relations of the display. For example, the simple display in Figure 1 has five usable dimensions: the vertical position of the ellipse within the field; horizontal position; the eccentricity or shape of the ellipse; the area or size of the ellipse and the angular orientation of the ellipse. In our example of the power plant, if the temperature of the steam is mapped into the vertical position and the pressure of the steam is given by the horizontal position, then the linear relations between these two variables are directly represented by positions along diagonal axes.

## Advantages and Disadvantages of Integrated Displays

This ability to directly represent relational information is the major advantage that is assumed to accrue from the use of integrated displays. However, in order to assess and maximize this advantage, we must confront two questions about the perceptual abilities of the human observer. First, can observers extract and utilize relational information? Only in the context of an affirmative answer to this question does the use of integrated displays seem reasonable at all. Second, in situations where relational information can be expected, to what extent does it obscure the original information about the separate variables on which it was based? In other words, can an integrated display be used in one moment to perceive relations among variables and in the next to obtain information about the variables themselves. Such display characteristics would be ideal; obviously the discovery of displays that come as close as possible to this ideal would be the goal of any research attempting to develop principles of display design.

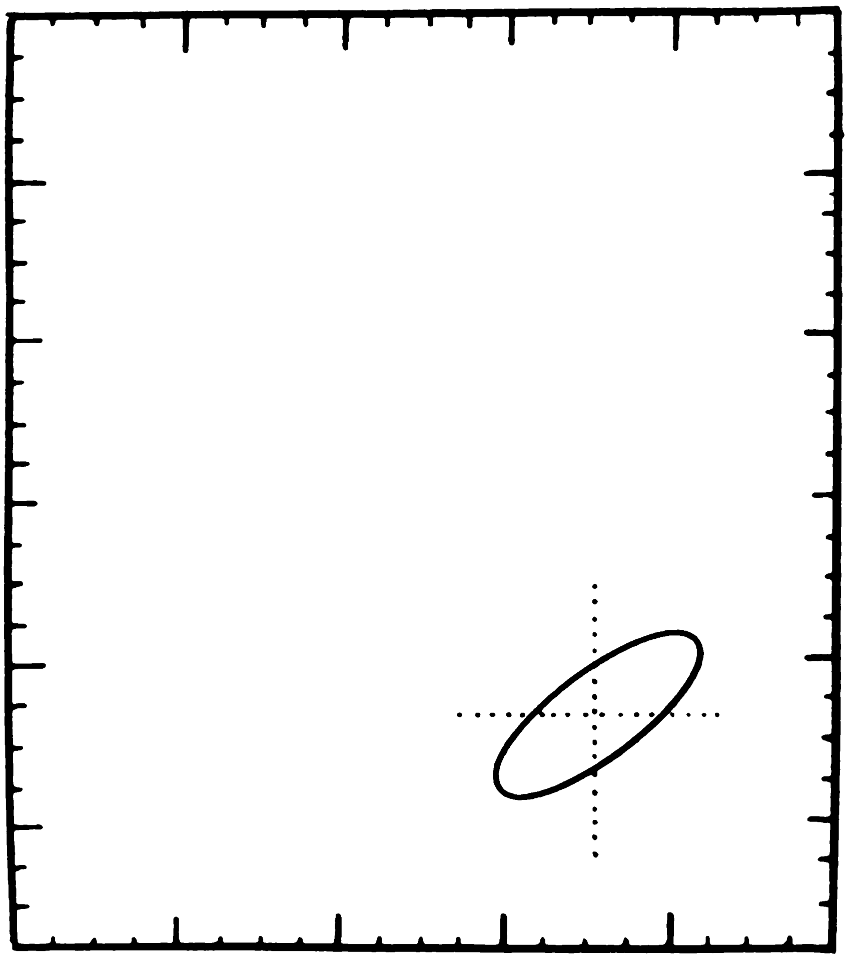

*Figure 1 — A simple five dimensional integrated display. The relevant dimensions are: the verticle and horizontal displacement of the ellipse; the angular orientation of the ellipse; and the size and eccentricity of the ellipse. Figure 6 — Multidimensional scaling plots for judgements of triangular patterns. Similarity is given by interpoint distances.*

The first of these questions can be answered with an unqualified yes. For suitable displays there is no doubt that an observer can extract relational information. In fact, the human perceptual system appears to be predominantly attuned to relational information. For example, the fact that we perceive objects in the real world to be of constant brightness, shape and size, in spite of the fact that the sensory information representing those objects is continually undergoing changes of luminance, orientation and projected size on the retina, is testimony to the relational sensitivity of the perceptual system. Furthermore, relational information is often more salient than information about unidimensional variables. Most people are quite poor at making absolute judgments about isolated variables. Thus, the use of integrated displays to represent relational information takes advantage of one of the basic perceptual talents of the human observer.

It would therefore be more valuable to rephrase our first question to ask under what conditions is the extraction of relational information optimal. the answer to this reformulated question reveals that optimizing the extraction of relational information can adversely affect the observer's ability to extract information about single variables. This is one of the major disadvantages of integrated displays. In the example illustrated by way of Figure 1 the dimensions of vertical and horizontal position seem to be independent of the representation of the relational information, the diagonal displacement. However, as we make these displays slightly more complex, or when we look at more complicated relations involving more than two variables, such independence is not so easily found. For example, the variables of ellipse size, shape and orientation in Figure 1 interact extensively, with judgments of area being much more difficult when eccentricity varies and judgments of eccentricity change as a function of orientation.

Furthermore, beside this potential distortion among correlated dimensions in an integrated display, there is the simple problem of distraction due to the presence of irrelevant information. That is, as we complicate displays to present more data we make it more difficult for the observer to pick out specified subsets of this information, to filter out the relevant from the irrelevant variables. Also when the extent that new features of a display emerge as the result of presenting configurations of separate features, the potential for distraction goes even beyond those aspects of the display that were added to convey simple information. Thus, the more directly perceivable the relational information in a display is, the more it can interfere when the observer is attempting to attend to the more simple levels of information.

## The Concept of Integrality

This tradeoff between the perception of relational properties and the ability to judge individual dimensions of a display is related to an old problem in psychology—phenomenologically, visual patterns seem to be qualitatively different with regard to the degree to which their component elements remain identifiable. Certain visual patterns appear to be heavily determined by the relations among their physically independent attributes. For many figures the physical attributes seem hardly identifiable at all. The patterns are perceivably only as unitary wholes. For other patterns the component dimensions remain readily apparent. The relations among the attributes can only be cognitively determined. These two circumstances define a continuum, which may be called "integrality," or the extent to which a pattern's physically definable attributes coalesce into a unitary whole figure.

The concept of integrality can be used to describe the relationship noted in the previous section. The disadvantages due to distortion and distraction that accrue to highly relational displays are typical of the problems of integral patterns. In general, the more a pattern is dependent upon relations for its definition, the more obscure are its component features, and certainly then, the less available will be those features for conveying information about a system for which the pattern is serving as a representation. Thus, the concept of integrality indicates that the efficacy of integrated displays will depend upon the task that the observer is undertaking. For making decisions based on relations, integral patterns will be good. On the other hand, for attending to component attributes integral patterns are not good. If, however, a display is to be used for both purposes, then the ideal pattern type ought to be one which has some degree of integrality but in which the component parts retain some measure of identifiability.

Figure 2 illustrates some of these ideas. Pattern 2a is generated by six vectors emanating from a point. The length of each of these vectors could be used to represent the magnitude of some variable of a complex system. In this pattern the attributes are reasonably apparent and the display would not be considered particularly integral. Pattern 2b is also generated by six vectors emanating from a single point. In this case, however, the end points of the factors have been connected to form a six-sided geometric figure. It seems to have no separately identifiable features, but rather seems perceivable only as a unitary figure. The specific form of the geometric pattern, the property that differentiates it from other patterns generated in the same way, is the relations among the six vectors, even though the vectors are not visually apparent. Thus, with regard to the generating vectors, this figure represents solely relational information.

Figure 2c illustrates yet another type of integrated display. Here information about a system would be mapped into the various features of the schematic facial drawing. These features include the shape and the slant of the eyes, the curvature and the size of the mouth, the size of the nose and the outline shape of the face. This figure has both integral and non-integral aspects. An observer can attend to and identify each of the features separately, yet together the features form a unitary and meaningful pattern. Correlations among variables become translated into salient characteristics of the face, such as its emotional expression. Expression thus becomes a feature of the pattern, even though no single feature of the system is being mapped into it. It emerges as a result of the particular configuration of the features that were used in its construction and the particular correlation of underlying system variables. Furthermore, expression is a highly reliable and identifiable feature. For example, we have shown patterns of this type to observers in which we have varied all of the separate features across their permissible ranges and found almost complete agreement among the observers in their descriptions of the facial expression. Thus, this emergent property, which is determined by the relations among the separate features, can be a reliable source for the transmission of information about a complex system.

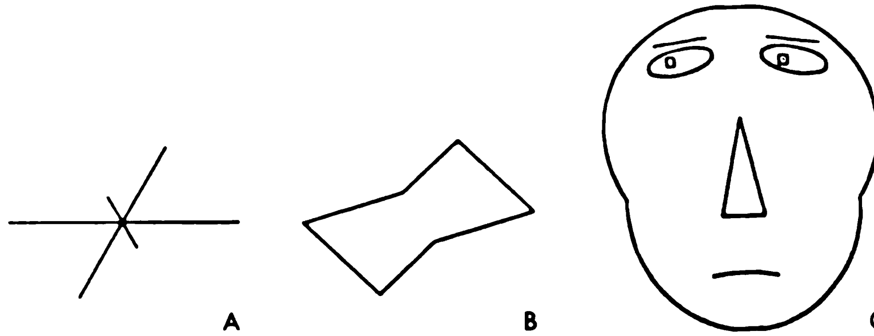


*Figure 2 — Three integrated display types. Pattern A is low in integrality; Pattern B is high in integrality; Pattern C is intermediate in integrality.*

## The Measurement of Integrality

Figure 2c possesses those characteristics that could be termed moderate integrality: Observers can perceive the relational aspects of the figure, but the separate features remain identifiable. As noted above, however, we still must determine whether the identifiability of the features remains complete or whether the perceivable emergent property (facial expression) modifies or obscures the separate features. Clearly, the suitable application of integrated displays such as these will depend on the answer to this question.

We have recently developed techniques for investigating this question. The techniques are based on asking observers to rate the degree of similarity between two patterns with regard to particular selected features. Other features of the patterns are controlled (i.e. held constant) or are varied systematically. The use of similarity judgments allows us to measure perceptual distortion of the relevant features due to the variation of features irrelevant to the judgments. If observers can ignore the variation of the irrelevant features, the perceived similarities between patterns will resemble those in the contol condition, where the irrelevant features are held constant. If such selective attention is impossible, the influence of the irrelevant dimension will be revealed in the pattern of similarity judgments. According to the notion of integrality developed above, observers will be unable to ignore irrelevant features that are integral with relevant ones. In fact, the degree of interference due to the variation of irrelevant features can be used as a measure of integrality.

Figures 3 and 4 present typical data for one observer. In this experiment the subject was asked to rate the similarity of schematic faces with regard to the shape of the facial outline. In the control condition facial expression was not allowed to vary. In the experimental condition facial expression varied, but the subject was instructed to ignore it. The numbers in Figure 3 and 4 are labels for the individual schematic faces that were used in the experiment. The figures summarize the similarity ratings for pairs of faces by representing similarity as interpoint distances. Consequently, faces that were judged to be similar (e.g. faces

12 and 16 in Figure 3) will be close to each other, while faces judged to be dissimilar will be far apart (e.g. faces 9 and 4 in Figure 3). Figure 3 presents the control condition, in which facial expression was not varied. Figure 4 presents the experimental condition. The faces whose numbers are circled were given one facial expression while those represented by uncircled numbers were given a different expression. Note again that the subject was asked simply to judge the similarity of the shapes of the faces in both conditions.

A comparison of Figures 3 and 4 shows that varying facial expression had large and systematic effects on the judged similarity of shape for this observer. In Figure 4, faces with common expressions are grouped together. The average similarity for pairs within the groups is far greater than the average similarity of pairs from different groups. The observer was simply unable to ignore the facial expression and his rated similarity of facial shape was influenced by this irrelevant information. For example, faces 10 and 6 have quite similar shapes, as shown by their proximity in the control condition. In the experimental condition, where they vary in expression, their shapes are perceived to be much less similar. Thus, although there is a degree of identifiability

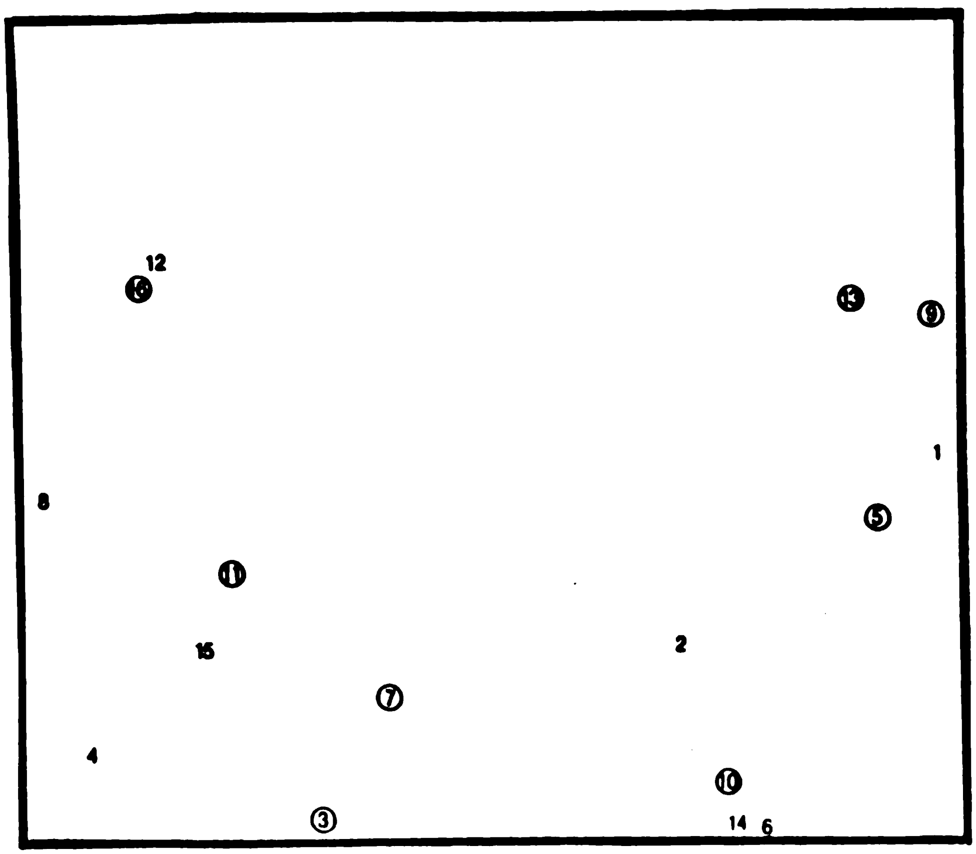


*Figure 3 — Multidimension scaling plot for sixteen patterns in the control condition (facial expression held constant). The rated similarity for two patterns is given by the interpoint distance.*

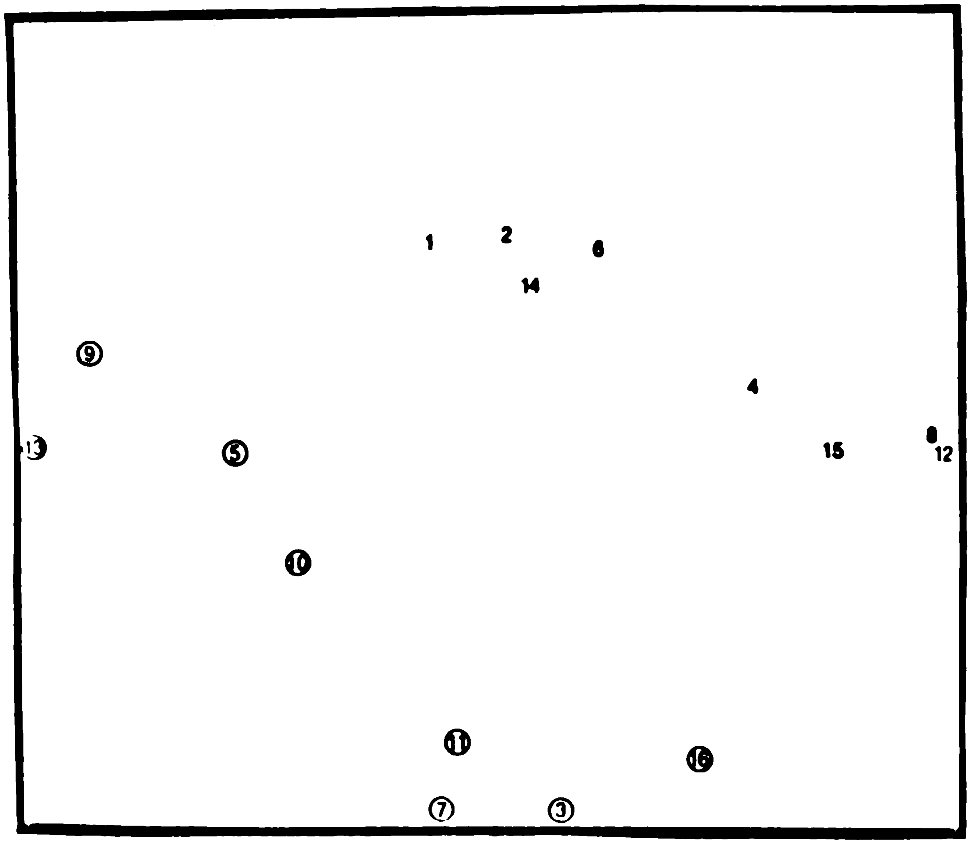


*Figure 4 — Multidimensional scaling plot for the experimental condition. Patterns whose numbers are circled had one facial expression, while those that are uncircled had a different facial expression.*

to the separate features for coherent diagrams such as these schematic faces, such attributes can be shown to be integral.

Furthermore, the degree of integrality can be measured directly from Figures 3 and 4. This is done by computing the ratio of the average interpoint distance among faces with similar expressions to the average interpoint distance between faces with different expressions, in the experimental condition. The ratio of the analogous distances in the control condition serves as a baseline, since the outline shapes are identical to those in the experimental condition, but facial expression does not vary. Comparing the ratios for the two conditions yields a continuous quantitative scale of integrality.

## The Psychophysics of Integrality

We have thus far argued that a critical concept with regard to the development of integrated multidimensional displays is the concept of display integrality. We have presented examples of display types that are more or less integral and we have demonstrated the damaging effects of integrality on the ability of observers to ignore irrelevant information. Furthermore, we have shown that we can measure the degree of integrality for a given display type. None of this, however, tells us what integrality is, how it comes about, or what can be done about it with regard to constructing integrated displays. These questions must be answered before meaningful applications of our concepts can be made. In short, we need a theory about integrality. In this section we will outline briefly the beginnings of such a theory, which we hope will speak to these issues. Of perhaps greatest importance is the fact that the theory shows that any given display type can be made to be more or less integral by simply manipulating the function that maps the components of the system to be represented into the physical dimensions of the display. That is, our theory asserts that much of the interfering effect of integrality can be eliminated by means of an appropriate definition of the physical parameters of the display pattern.

First, note that any pattern or display type can have any number of potential descriptions. For example, we could describe Figure 2c by saying that the eyes are ellipses with a height to width ratio of .39, slanting 12 degrees below the horizontal drawn at the inner point of the eye; that the slant of the eyebrows is eight degrees, and that the mouth is composed of the upper 25 degrees of a circle whose radius is equal to the height of the face. We could alternatively say that this face is somewhat sad. Similarly, we could note that the polygon in Figure 2b was generated by connecting the end points of six regularly spaced vectors emanating from a single point. Or, we could describe the polygon in terms of its jaggedness, elongation, size, symmetry and regularity. In both cases the first description makes use of dimensions that are more or less arbitrary, a particular physical description of the pattern. The second description, on the other hand, probably corresponds more closely to the perceived characteristics of the figure, its psychological attributes. If we could describe a pattern purely in terms of its psychological dimensions, that is, if we could come up with a physical description whose components correspond exactly to the perceived attributes, then the problem posed by integrality would disappear. Integral dimensions are, by definition, those that are not easily treated separately by the observer. Since the psychological dimensions are those different aspects of the pattern that the perceiver notices, they must be separable or non-integral. Thus the integrality of display dimensions is the result of our having chosen to talk about physical dimensions that combine or cut across psychological attributes. The degree of integrality can be defined as the degree to which the physically specified dimensions lack correspondence with the psychological dimensions.

The task, then, of designing a display whose purpose is to integrate information about a complex system involves, not so much the measurement of the integral properties of an arbitrarily chosen set of physical dimensions, but rather, the determination of the perceptually salient features of the display and their physical description. A psychophysically compatible mapping of system variables into pattern characteristics can then be produced. A display pattern determined in this fashion would have characteristics that earlier were termed to be ideal: Relational information would be presented in the form of an integrated display; however, the component attributes would be independently identifiable and would not interfere with each other.

## The Determination of Psychophysical Compatibility

How can such compatible formats be arrived at? As in the case of measuring the degree of integrality for arbitrarily designated physical dimensions, we can utilize the techniques of modern multidimensional psychophysics. Again we ask the observers to rate the perceived similarity of pairs of displays. These judgments are then submitted to a mathematical analysis that converts these ratings into the psychological "distances" between the displays. A map of these distances (i.e. a spatial arrangement of the points) will then represent the psychological structure of the entire set of displays.

For example, consider the simple triangular forms of Figure 5. These forms are constructed with a common base. That is, the length and orientation of the base is held constant. Therefore, there are only two degrees of freedom of physical variation among the set of displays, so that any particular pattern can be uniquely specified by a minimum set of two physical parameters. There are, however, many different pairs of parameters that could be used to describe these triangles. In Figure 5 for example, the differences among the 13 patterns presented are designated as height (the vertical distance of the vertex to the base line) and angle (the number of degrees in the interior obtuse angle). Alternatively, these patterns could be uniquely specified by their area and the length of one of the freely varying sides, or the lengths of the two freely varying sides, or two interior angles, etc. All of these descriptions are equivalent for the purposes of the physical specification of the patterns.

Our goal is to find the physical description that most closely describes the most perceptually salient attributes of the patterns. Let us consider height and angle. The four triangles in figure 5 were chosen as orthogonal examplars of these dimensions. That is, the triangles in each row have equal values for the interior obtuse angle, and the triangles in each column have equal heights. However, as perceptual variables the differences in these variables do not look independent. In fact, we have asked observers to judge the similarity of the pairs on the diagonal, that is, on the one hand the pair 1 and 4, and on the other hand, the pair 2 and 3. Invariably observers will note that the pair 2 and 3 look more similar to each other than pair 1 and 4. Note, however, that in terms of the physical differences these two pairs are equally different. It is this lack of correspondence between physical and psychological variables that we have termed integrality because it is clear that the overall similarity of the figures is a joint function of height and angle. Thus, these variables can not be separated easily by the observer.

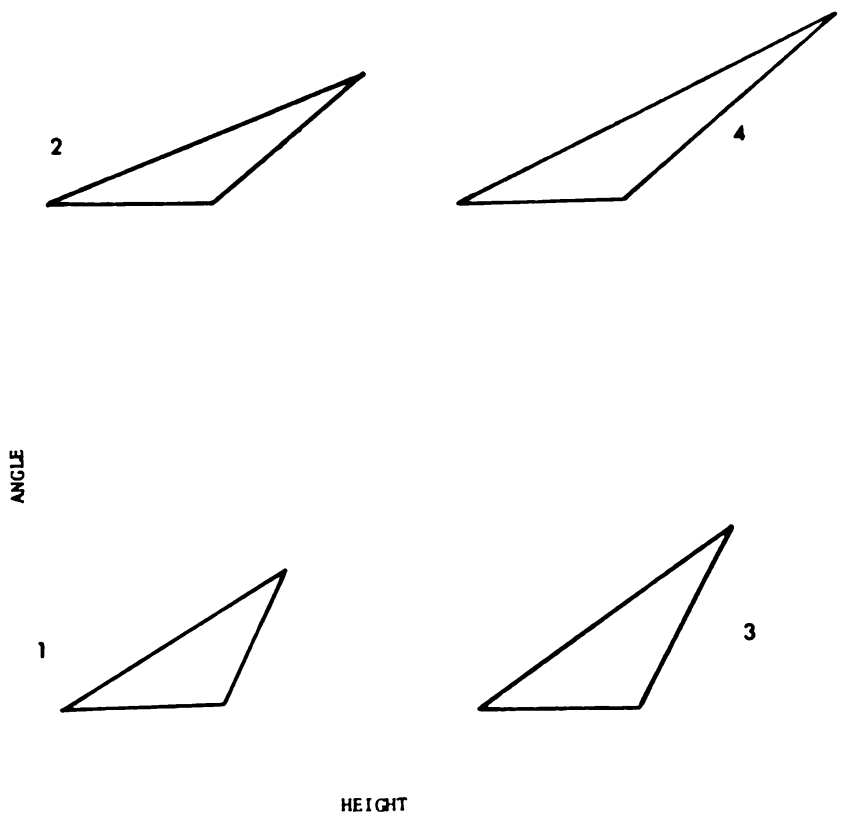


*Figure 5 — Four triangular patterns that differ orthogonally in height and size of the interior obtuse angle.*

In an effort to discover a set of dimensions corresponding more closely to the psychological attributes for this pattern type, we developed a larger set of triangles. for values of height and, instead of angle, four values of the length of the right side were orthogonally combined to create a set of sixteen patterns. Observers were then asked to make similarity ratings for each of the possible pairs of triangles within the set. These ratings were then mathematically transformed into a picture of the psychological distances between the patterns. Figure 6a shows the typical data of one subject. The solid lines connect triangles that differ from each other only in terms of height (they are equal in length of side). If there had been a high compatibility between these physical dimensions and the perceiveable attributes of the figures, this figure would have been rectangular. As in the case of triangles varying orthogonally in height and angle, however, the pattern of perceived similarities differed markedly from that expected if judgments were based on the orthogonal dimensions. For this observer the violation of rectangularity is roughly multiplicative. That is, the overall similarity of the triangles is a function of the product of height and angle.

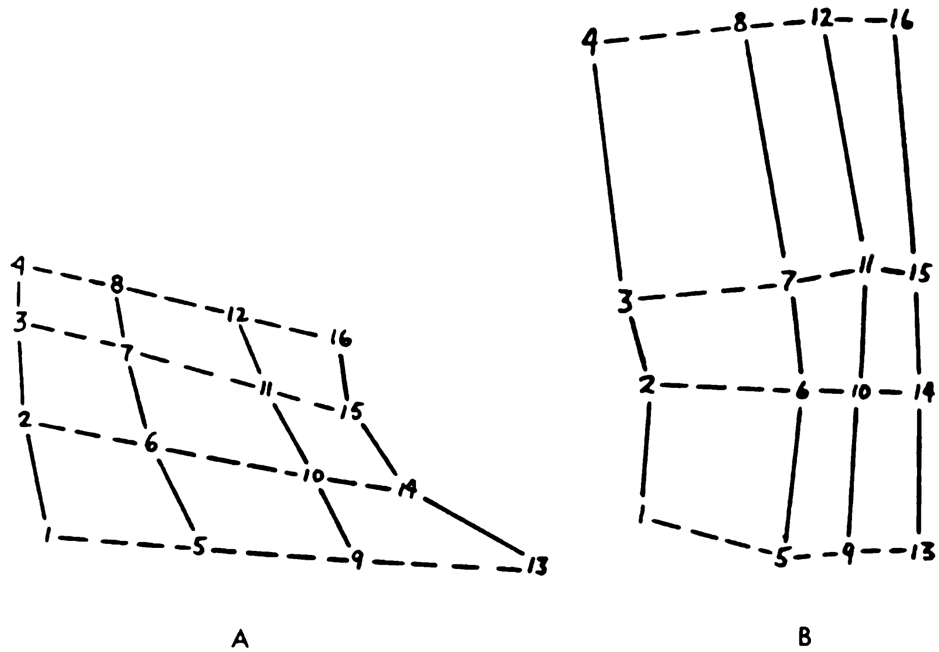


*Figure 6 — Multidimensional scaling plots for judgements of triangular patterns. Similarity is given by interpoint distances.*

This fact can be used to construct sets of displays that will be high in psychophysical compatibility. For example, we constructed a set of sixteen triangles that differed from each other orthogonally in terms of the product of height and length of the right side, on the one hand, and in terms of angle on the other. The data in figure 6b show the psychological "map" of the interpoint similarities for the same observer whose data were shown in figure 6a. Again, the solid lines connect triangles that differ from each other only in terms of the product of height and side. The dotted lines connect points that differ only in terms of angle. It is clear that this manipulation has removed the interaction that was present in figure 6a. Thus, these variables could be used to produce non-interfering mappings of information about two aspects of some complex system.

## Conclusions

The methodology illustrated above, we believe, represents a general solution for the discovery of compatible psychophysical relations. Generally, one needs to carefully examine data like that presented in figure

6. In most cases it is reasonable to expect that more complicated "correcting functions" will be needed than the simple mutliplicative function discovered here. However, even in very complicated circumstances, data such as those from the present example could be simply entered into a computer and appropriate interpolation of the points could be used to generate required displays. Given the great flexibility of modern computerized display devices, one could even conceive of the possibility that different appropriate mappings could be achieved for individual observers.

There are some important limitations to the present research that need to be noted. All of the concepts presented in this paper have concerned themselves solely with the psychophysical aspects of display design. That is, they have been concerned with the way the displays appear to the observer. There is, of course, the strong presumption that the appearance of displays will determine to a great extent the nature of the performance of observers who are dealing with them. There are, however, a number of additional factors involved in a performance situation that are not entailed in a simple judgment of similarity. The most striking difference between the two situations is in the nature of the response required: in a realistic setting an observer must make a response that can be objectively judged right or wrong. Our ability to predict the quality of an observer's performance from data about the appearance of a display depends to a large extent on the relevance of similarity judgments to judgments of specific values on the dimensions of the display.

Initial research indicates that this relationship is a valid one. Violations of rectangularity in similarity judgments are accompanied by an inability to correctly classify values of single dimensions when the observer is under speed stress. Further research is under way to determine whether patterns of similarity judgments can be used to predict patterns of performance in the speeded task.

In addition to the nature of the response required, other variables in a performance situation could affect the ability of the observer to utilize information presented in a display. These include the amount of speed stress he is under (i.e. the degree to which fast responding is stressed over accuracy or vice versa) and the cognitive requirements of the task. By cognitive requirements, we refer to the possibility that, besides simply determining what information is being presented in the display, the observer may have to compare this information to information being held in memory or perform some transformation of the information to reach a decision.

The accurate performance of all of these tasks, however, is based on the accurate perception of the information presented. Thus, while additional research is needed that incorporates psychophysically compatible and incompatible displays into actual performance situations, we expect that the quality of an observer's performance can ultimately be predict-ed from psychophysical data. When this stage has been reached, the construction of optimal integrated multidimensional displays will be a matter of implementing the mapping of system variables into the display parameters that are most compatible with the observer's perceptual system.

---

## Elastic Deformation of the Earth and Its Relation to the Shape of the Earth and Tide Determination

The determination of the shape of the earth and of the periodic motion of the ocean mass is a fundamental problem that has attracted the interest of scientists for a long time.

The recent advent of large computers has rendered feasible the numerical solution of more complicated mathematical models of the physical problem. In the determination of the shape of the earth, the fundamental approach has been to sense the variation of the gravity field of the earth from the normal field generated by a simple geometrical surface of reference: this can be achieved by means of measurements performed on the solid ground or on board a ship.

Artificial satellites have also been used to determine the gravity potential of the earth by means of ground stations tracking the satellite and ascertaining the perturbations suffered by its orbit from a theoretical solution.

A more recent endeavor has been the use of radar altimeters located on satellites to determine the distance from the satellite to the crest of the ocean waves. The full use of this data necessitates a realistic model of the global ocean tides.

Paolo Lanzano and John Daley, scientists at the Naval Research Laboratory, have been spearheading a new approach which consists of determining the deformation of the earth; fortunately, the internal constitution of the earth can be derived from earthquake data.

Until now, density models and deformation profiles have been obtained by ignoring the perturbing effects of the earth's rotation. The NRL team has developed a mathematical model that takes the rotational motion into account.

Although more complicated in solving, the new set of equations should provide a more refined reference surface; this ultimately will lead to a more accurate measurement of the earth's shape using the present state-of-the-art in gravity measurements. Use of this approach is also expected to help improve the mathematical model of the ocean tides by introducing refinements, such as taking into consideration the self-gravitation of the ocean mass and the deformation of the ocean bottom due to the inhomogeneity of the earth; the latter input stems directly from the present effort.

An accurate mathematical model of the tidal problem which is still compatible with the constraints of the present generation of computers and which is complementary to the ocean measurements data should lead to a knowledge of the equilibrium surface of the ocean down to the ten-centimeter level as it is required for future oceanographic applications.



U. S. GOVERNMENT PRINTING OFFICE: 1979 O - 290-987

# Cryogenic Cooler for Ship Propulsion Systems

A novel helium liquefier, a refrigeration device designed to provide the thermal environment needed for the superconductive motors and generators to be used in some Navy ship propulsion systems in the future, has been developed by Dr. Samuel C. Collins at the Naval Research Laboratory. The invention was developed as part of a research effort in cryogenics sponsored by the Naval Ship Research and Development Center (NSRDC) at Annapolis, Md.

NSRDC is attempting to adapt superconductive motors and generators for ship propulsion uses in the Navy's new, fast surface effects ships. These machines must operate at a temperature only a few degrees above absolute zero (−459.4F).

Dr. Collins, who also invented an airborne oxygen liquefier for aircraft and the Collins Cryostat (the first commercially feasible helium liquefier), reports his new liquefier is 20% more efficient and is smaller than other liquefiers presently available, and it is made to withstand heavy shocks.

Two models of Collins' liquefier have been sent to NSRDC for operational reliability tests. One is a three-cylinder engine for the expansion of helium at three temperature levels with a 5-10 liter capacity per hour. The second has a four-cylinder engine, with an extra-large bore and stroke on one of the cylinders for use during the cool-down period only. Its capacity is 10-20 liters, with the yield being determined by the speed at which the engine is operated.

---

**NAVAL RESEARCH REVIEWS** publishes highlights of research conducted by Navy laboratories and contractors and describes important naval experimental facilities. Manuscripts submitted for publication, correspondence concerning prospective articles, and changes of address, should be directed to Code 730, Office of Naval Research, Arlington, Va. 22217. Requests for subscriptions should be directed to the Superintendent of Documents, U.S. Government Printing Office, Washington, D.C., 20402. Subscription price: $11 per year in the U.S. and Canada; $13.75 per year, foreign; $1 per individual copy. The issuance of this periodical approved in accordance with Dept. of the Navy publications and printing regulations.

*Editor:* WILLIAM J. LESCURE

NAVSO P-510

*Associate Editors:*

**L. LARMORE, ONR PASADENA**
**G. SANDOZ, ONR CHICAGO**
**A.L. POWELL, ONR BOSTON**
**D.A. PATTERSON, NAVAL RESEARCH LABORATORY**

# IN THIS ISSUE

VOL. XXXI NO. 11



## Cover Caption

*This display panel in the cockpit of the F/A-18A aircraft is now being tested. Note the head up display on the windshield with its coding dimensions of the speed, angle, height, and other status indicators of the aircraft in relation to the terrain.* **(see page 19)**

**DEPARTMENT OF THE NAVY**
**OFFICE OF NAVAL RESEARCH**
**ARLINGTON, VA. 22217**

**OFFICIAL BUSINESS**

*PENALTY FOR PRIVATE USE, $300.*

**POSTAGE AND FEES PAID**
**DEPARTMENT OF THE NAVY**
**DoD-316**
CONTROLLED CIRCULATION RATE

U.S.MAIL